Electronic Supplementary Material (ESI) for Dalton Transactions.

Supporting Information

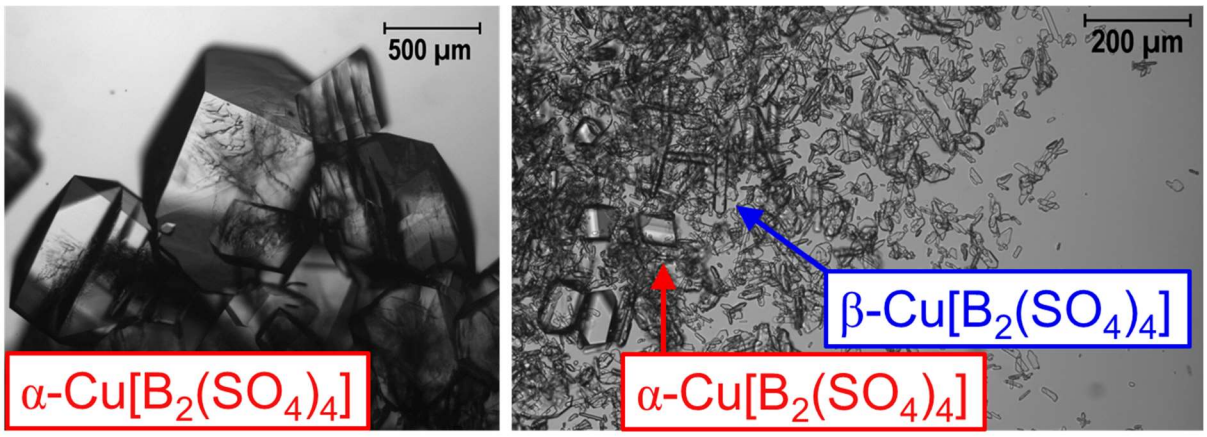

Fig. S1. Microscope pictures of α-$Cu[B_2(SO_4)_4]$ (left, through closed ampoule) and β-$Cu[B_2(SO_4)_4]$ (right, embedded in perfluorinated polyether) showing the morphology of the crystals and the presence of α-$Cu[B_2(SO_4)_4]$ crystals in the β-$Cu[B_2(SO_4)_4]$ sample.

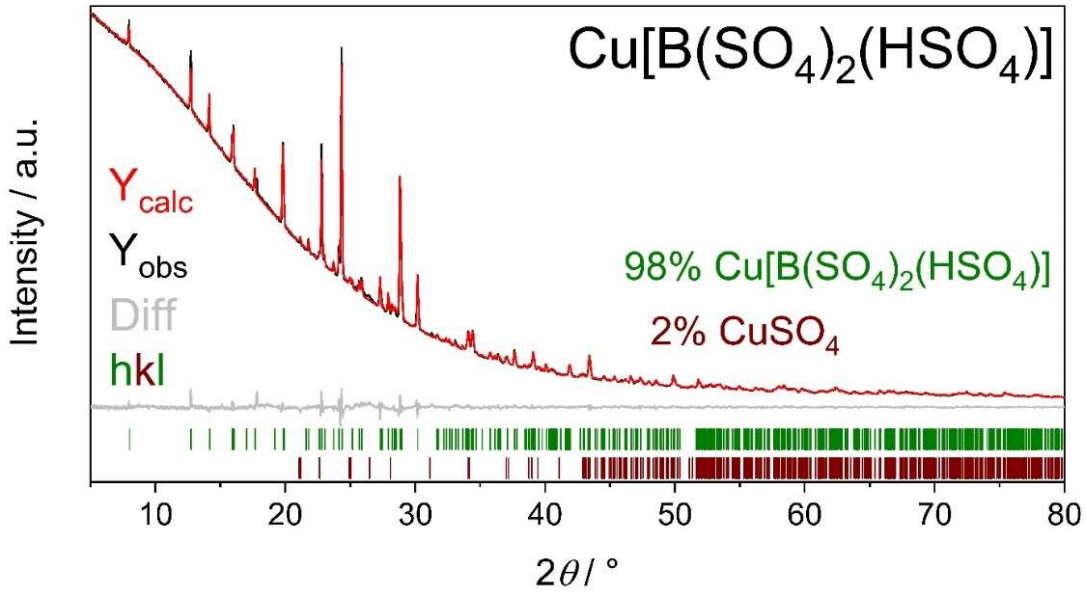

Fig. S2. Rietveld-Refinement of $Cu[B(SO_4)_2(HSO_4)]$ showing contents of 98% for the main phase $Cu[B(SO_4)_2(HSO_4)]$ and 2% for the side phase $CuSO_4$. Further details can be found in Table S2.

Table S1. Crystal data and structure refinements of α-$Cu[B_2(SO_4)_4]$ and β-$Cu[B_2(SO_4)_4]$ determined from powder XRD data via Rietveld refinement[a]

	α-$Cu[B_2(SO_4)_4]$	β-$Cu[B_2(SO_4)_4]$[b]
CSD number	2118182	2118180
M / g mol^{-1}	469.40	
Temperature / K	300(2)	
Space group	$P\bar{1}$ (no. 2)	$P2_1/n$ (no. 14)
a / pm	526.36(2)	772.63(1)
b / pm	714.49(2)	813.14(1)
c / pm	793.52(2)	906.64(1)
α / °	73.698(2)	90
β / °	70.737(2)	111.132(1)
γ / °	86.677(2)	90
Volume / 10^6 pm^3	270.19(1)	531.30(1)
Z	1	2
R_{Bragg}	0.005	0.004
ρ_{calcd} / g cm^{-3}	2.885	2.934
Radiation; wavelength λ / Å	Cu$K\alpha$; 1.54184	
Diffractometer	Bruker D8 Advance	
2θ range / deg	5–80	
No. of independent parameters	65	64
R_p	0.006	0.005
R_{wp}	0.009	0.008
GOOF	1.99	1.82

[a] The respective standard deviations are given in parentheses. [b] β-$Cu[B_2(SO_4)_4]$ was refined with a 7 wt.-% side phase of α-$Cu[B_2(SO_4)_4]$ (R_{Bragg} = 0.006) taking the results of the refinement on α-$Cu[B_2(SO_4)_4]$ as fixed values.

Table S2. Crystal data and structure refinements of $Cu[B(SO_4)_2(HSO_4)]$ determined from powder XRD data via Rietveld refinement[a]

	$Cu[B(SO_4)_2(HSO_4)]$
M / g mol^{-1}	363.54
Temperature / K	300(2)
Space group	$P\bar{1}$ (no. 2)
a / pm	533.32(2)
b / pm	707.36(3)
c / pm	1130.6(1)
α / °	81.271(2)
β / °	80.205(3)
γ / °	81.141(2)
Volume / 10^6 pm^3	411.82(3)
Z	2
R_{Bragg}	0.009
ρ_{calcd} / g cm^{-3}	2.932
Side phase	$CuSO_4$
Space group	*Pnma* (No. 62)
a / pm	842.2(2)
b / pm	672.80(2)
c / pm	482.99(2)
Volume / 10^6 pm^3	273.7(1)
Z	2
Fraction of side phase / wt.-%	2
Radiation; wavelength λ / Å	Cu$K\alpha$; 1.54184
Diffractometer	Bruker D8 Advance
2θ range / deg	5–80
No. of independent parameters	82
R_p	0.008
R_{wp}	0.015
GOOF	2.77

[a] The respective standard deviations are given in parentheses.

Table S3. Crystal data and structure refinements of $Cu(HSO_4)_2$-I and $Cu(HSO_4)_2$-II determined from single crystal XRD[a]

	$Cu(HSO_4)_2$-I	$Cu(HSO_4)_2$-II
CSD number	2118185	2118183
M / g mol^{-1}	257.68	
Crystal size / mm^3	0.3 × 0.2 × 0.2	0.8 × 0.4 × 0.4
Temperature / K	293(2)	
Space group	$P2_1/n$ (no. 14)	$P\bar{1}$ (no. 2)
a / pm	475.30(2)	479.88(8)
b / pm	853.25(4)	785.67(13)
c / pm	737.19(3)	805.66(14)
α / °	90	77.86(1)
β / °	100.063(1)	87.02(1)
γ / °	90	89.82(1)
Volume / 10^6 pm^3	294.37(2)	296.55(9)
Z	2	
ρ_{calcd} / g cm^{-3}	2.907	2.886
Absorption coefficient μ / mm^{-1}	4.42	4.39
F(000) / e	254	254
Radiation; wavelength λ / Å	Mo$K\alpha$; 0.71073	
Diffractometer	Bruker D8 Venture	
θ range / °	3.685– 32.484	2.590–24.987
Absorption correction	Multi-scan	
Transmission (min; max)	0.6892; 0.7490	0.6237; 0.7453
Index range $h\|k\|l$	±7|±12|±11	±5|±9|±9
Reflections collected	9734	6430
Independent reflections	1063	1044
Obs. reflections ($I > 2\ \sigma(I)$)	1009	931
Refined parameters / restraints	55 / 1	109 / 2
R_{int}	0.032	0.045
R_1	0.019	0.048
wR_2	0.052	0.132
GooF	1.175	1.063
Residual electron density (max; min) / e^- Å^{-3}	0.45; -0.65	1.76; -0.86

[a] The respective standard deviations are given in parentheses.

Table S4. Wyckoff symbol, atomic coordinates *x*; *y*; *z* and equivalent isotropic displacement parameters U_{eq} and anisotropic displacement parameters U_{ij} in Å^2 for $Cu(HSO_4)_2$-I[a]

Atom	Wyckoff symbol	*x*	*y*	*z*	U_{eq}	U_{11}	U_{22}	U_{33}	U_{23}	U_{13}	U_{12}
Cu1	2*d*	1	½	½	0.00780(7)	0.00563(11)	0.00813(11)	0.00989(12)	-0.00306(7)	0.00204(8)	-0.00054(7)
S1	4*e*	0.44306(7)	0.33175(4)	0.28612(4)	0.00679(8)	0.00623(14)	0.00620(14)	0.00794(14)	-0.00200(10)	0.00122(10)	-0.00043(10)
O1	4*e*	0.4135(2)	0.16844(12)	0.23302(15)	0.0125(2)	0.0167(5)	0.0067(4)	0.0147(5)	-0.0042(4)	0.0047(4)	-0.0019(4)
O2	4*e*	0.7407(2)	0.38159(14)	0.31308(16)	0.0147(2)	0.0083(4)	0.0209(5)	0.0158(5)	-0.0092(4)	0.0048(4)	-0.0066(4)
O3	4*e*	0.3122(2)	0.36582(12)	0.44697(14)	0.00999(18)	0.0094(4)	0.0114(4)	0.0100(4)	-0.0015(3)	0.0038(3)	0.0021(3)
O4	4*e*	0.2809(3)	0.42088(14)	0.11773(15)	0.0160(2)	0.0210(5)	0.0158(5)	0.0105(4)	0.0026(4)	0.0007(4)	0.0064(4)
H1	4*e*	0.226(6)	0.5200(17)	0.164(3)	0.019						

[a] The respective standard deviations are given in parentheses.

Table S5. Wyckoff symbol, atomic coordinates *x*; *y*; *z* and equivalent isotropic displacement parameters U_{eq} and anisotropic displacement parameters U_{ij} in Å^2 for $Cu(HSO_4)_2$-II[a]

Atom	Wyckoff symbol	*x*	*y*	*z*	U_{eq}	U_{11}	U_{22}	U_{33}	U_{23}	U_{13}	U_{12}
Cu1	1*g*	0	½	½	0.0114(3)	0.0071(5)	0.0132(6)	0.0146(6)	-0.0047(4)	-0.0013(4)	0.0032(4)
Cu2	1*b*	0	0	½	0.0148(3)	0.0094(6)	0.0143(6)	0.0199(6)	-0.0019(5)	0.0000(4)	-0.0023(4)
S1	2*i*	0.1017(3)	0.31277(19)	0.19377(19)	0.0109(4)	0.0098(8)	0.0083(8)	0.0149(8)	-0.0032(6)	0.0008(6)	0.0021(6)
S2	2*i*	0.4602(3)	0.21874(19)	0.65355(19)	0.0103(4)	0.0075(7)	0.0074(8)	0.0167(8)	-0.0042(6)	0.0002(6)	0.0020(6)
O11	2*i*	0.2514(9)	0.3543(6)	0.0294(6)	0.0164(10)	0.019(2)	0.010(2)	0.020(2)	-0.0047(18)	0.0023(18)	0.0007(18)
O12	2*i*	0.1510(9)	0.1355(6)	0.2813(6)	0.0183(10)	0.017(2)	0.011(2)	0.024(2)	0.0010(19)	0.0046(19)	0.0034(18)
O13	2*i*	0.1663(9)	0.4419(6)	0.2927(6)	0.0167(10)	0.013(2)	0.015(2)	0.024(2)	-0.0108(19)	0.0015(18)	-0.0015(18)
O14	2*i*	-0.2126(9)	0.3216(6)	0.1642(6)	0.0186(10)	0.011(2)	0.020(3)	0.027(3)	-0.008(2)	0.0000(19)	0.0013(18)
H1	2*i*	-0.368(11)	0.349(10)	0.239(8)	0.022						
O21	2*i*	0.2990(9)	0.3772(6)	0.6375(6)	0.0152(10)	0.012(2)	0.012(2)	0.022(2)	-0.0054(18)	-0.0025(18)	0.0044(18)
O22	2*i*	0.7238(9)	0.2409(6)	0.5546(6)	0.0148(10)	0.008(2)	0.010(2)	0.025(2)	-0.0035(19)	0.0037(18)	0.0005(17)
O23	2*i*	0.3013(9)	0.0720(6)	0.6235(6)	0.0192(10)	0.016(2)	0.012(2)	0.032(3)	-0.008(2)	-0.0033(19)	-0.0012(18)
O24	2*i*	0.5414(10)	0.1706(6)	0.8399(6)	0.0229(11)	0.029(3)	0.021(3)	0.020(3)	-0.007(2)	-0.005(2)	0.012(2)
H2	2*i*	0.416(14)	0.226(10)	0.914(8)	0.027						

[a] The respective standard deviations are given in parentheses.

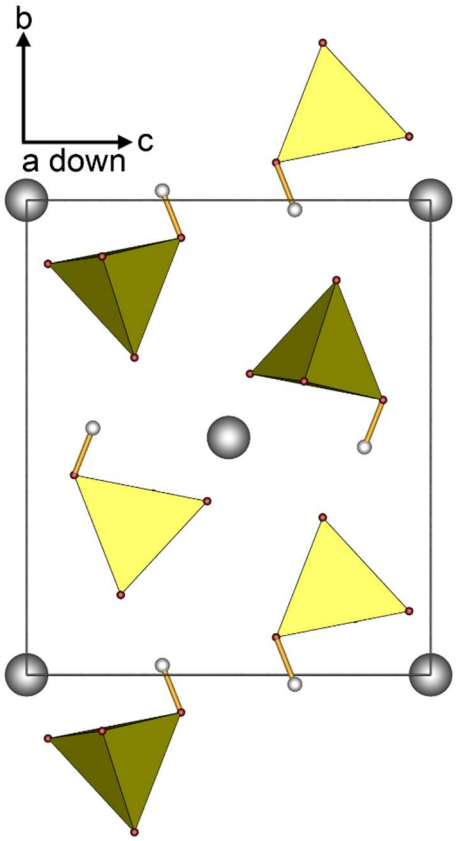

Fig. S3. Unit cell of $Cu(HSO_4)_2$-I viewed along (100); sulfate tetrahedra yellow, copper cations grey, oxygen atoms red; hydrogen atoms white.

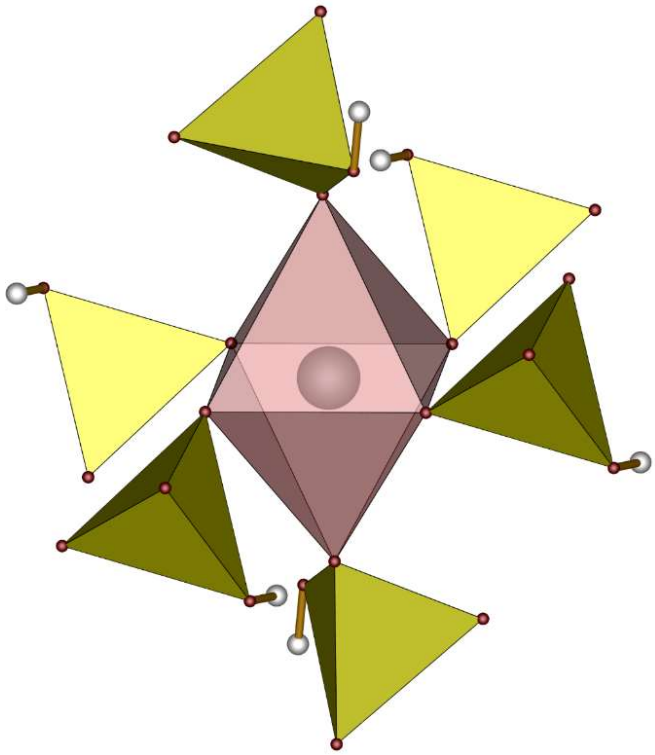

Fig. S4. Octahedral coordination environment of the Cu^{2+} cations (grey) in $Cu(HSO_4)_2$-I; sulfate tetrahedra yellow, copper cations grey, oxygen atoms red; hydrogen atoms white

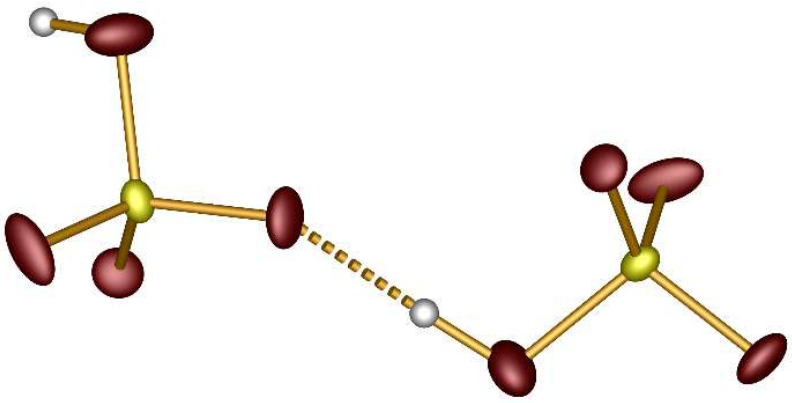

Fig. S5. Hydrogen bonding in $Cu(HSO_4)_2$-I; sulfur yellow, oxygen atoms red; hydrogen atoms white; the ellipsoids are shown at 80% probability.

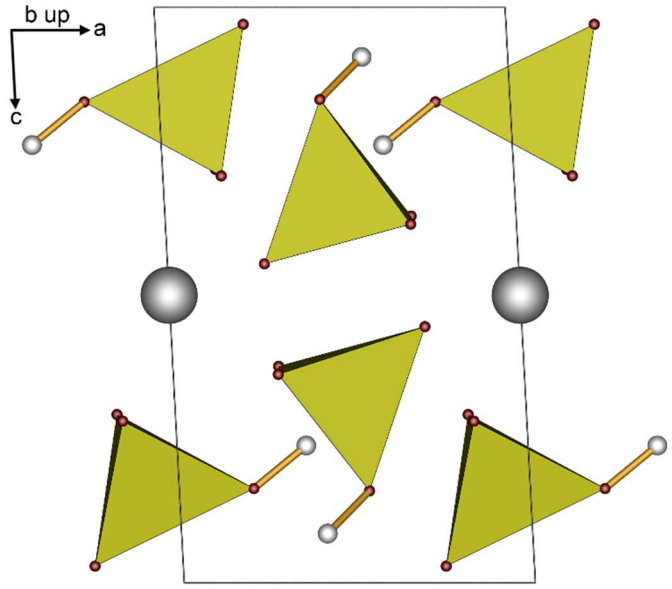

Fig. S6. Unit cell of $Cu(HSO_4)_2$-II viewed along (010); sulfate tetrahedra yellow, copper cations grey, oxygen atoms red; hydrogen atoms white.

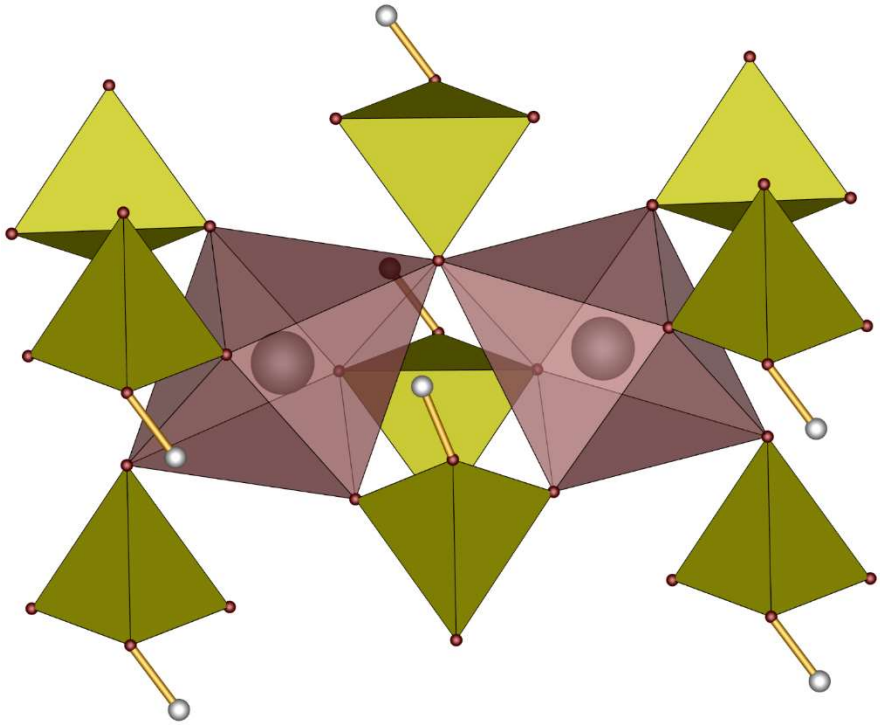

Fig. S7. Octahedral coordination environment of the Cu^{2+} cations (grey) in $Cu(HSO_4)_2$-II; sulfate tetrahedra yellow, copper cations grey, oxygen atoms red; hydrogen atoms white.

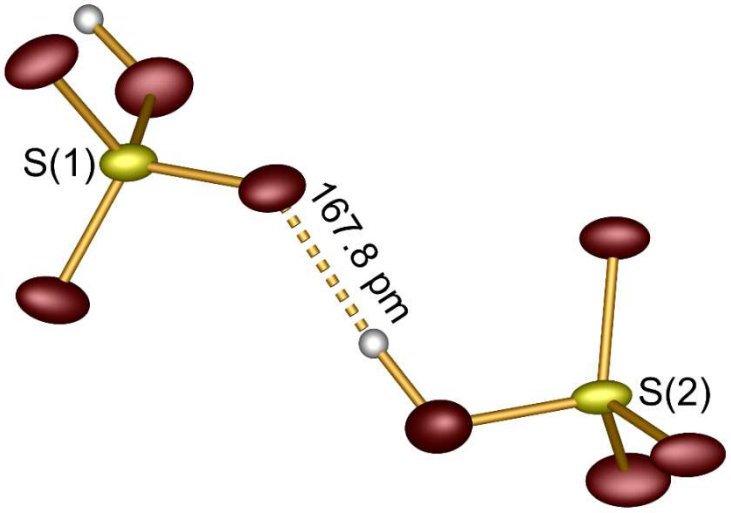

Figure S8. Hydrogen bonding in $Cu(HSO_4)_2$-II between $HS(1)O_4$ and $HS(2)O_4$ groups with O-H distance; sulfur yellow, oxygen atoms red; hydrogen atoms white; the ellipsoids are shown at 80% probability.

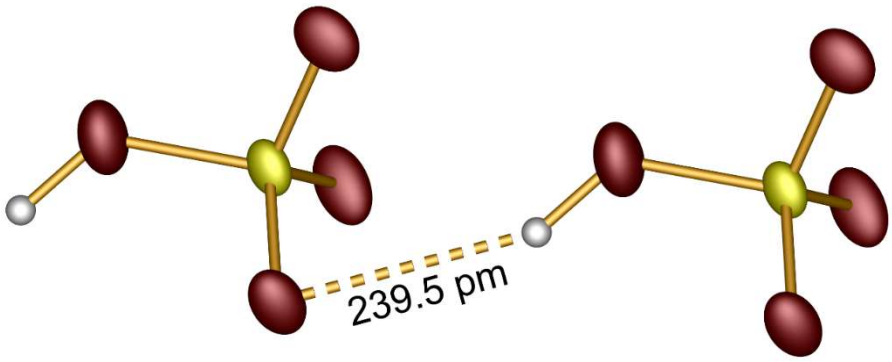

Figure S9. Hydrogen bonding in $Cu(HSO_4)_2$-II between two $HS(1)O_4$ groups with O-H distance; sulfur yellow, oxygen atoms red; hydrogen atoms white; the ellipsoids are shown at 80% probability.

Table S6. Electrostatic calculations for $Cu(HSO_4)_2$-I and $Cu(HSO_4)_2$-II.

$Cu(HSO_4)_2$-I	$CuSO_4^1 + SO_3^2 + H_2O^3$
MAPLE = 70334 kJ mol^{-1}	MAPLE = 70065 kJ mol^{-1}
	(Δ = 0.38%)
$Cu(HSO_4)_2$-II	$CuSO_4^1 + SO_3^2 + H_2O^3$
MAPLE = 70310 kJ mol^{-1}	MAPLE = 70065 kJ mol^{-1}
	(Δ = 0.35%)

Table S7. ECon derived by MAPLE-calculations for Cu atoms in $Cu(HSO_4)_2$-I

Atom	*x*	*y*	*z*	Distance / pm	Econ(1)	Econ(3)
Central atom						
Cu1	0	½	½			
Ligand						
O2	0.2593	0.6184	0.6869	196.087	1.093	1.108
O2	-0.2593	0.3816	0.3131	196.087	1.093	1.108
O3	-0.3122	0.6342	0.553	196.679	1.075	1.090
O3	0.3122	0.3658	0.447	196.679	1.075	1.090
O1	-0.0865	0.3316	0.733	233.072	0.208	0.216
O1	0.0865	0.6684	0.267	233.072	0.208	0.216
Next Ligand						
O4	-0.2809	0.5791	0.8823	339.036	0	0

Table S8. ECon derived by MAPLE-calculations for Cu(1) atoms in $Cu(HSO_4)_2$-II

Atom	*x*	*y*	*z*	Distance / pm	Econ(1)	Econ(3)
Central atom						
Cu1	0	½	½			
Ligand						
O13	0.1663	0.4419	0.2927	195.302	1.104	1.121
O13	-0.1663	0.5581	0.7073	195.302	1.104	1.121
O21	0.299	0.3772	0.6375	198.09	1.019	1.036
O21	-0.299	0.6228	0.3625	198.09	1.019	1.036
O22	0.2762	0.7591	0.4454	238.194	0.140	0.147
O22	-0.2762	0.2409	0.5546	238.194	0.140	0.147
Next Ligand						
O14	0.2126	0.6784	0.8358	349.52	0	0

Table S9. ECon derived by MAPLE-calculations for Cu(2) atoms in $Cu(HSO_4)_2$-II

Atom	*x*	*y*	*z*	Distance / pm	Econ(1)	Econ(2)
Central atom						
Cu2	0	0	½			
Ligand						
O23	-0.3013	-0.072	0.3765	194.738	1.072	1.081
O23	0.3013	0.072	0.6235	194.738	1.072	1.081
O12	-0.151	-0.1355	0.7187	196.103	1.03	1.040
O12	0.151	0.1355	0.2813	196.103	1.03	1.040
O22	0.2762	-0.2409	0.4454	240.965	0.096	0.099
O22	-0.2762	0.2409	0.5546	240.965	0.096	0.099
Next Ligand						
O14	0.2126	-0.3216	0.8358	348.419	0	0

Table S10. Crystal data and structure refinements of $Cu[S_2O_7]$ determined from single crystal XRD[a]

CSD number	2118184
M / g mol^{-1}	239.66
Crystal size / mm^3	0.06 × 0.05 × 0.03
Temperature / K	200(2)
Space group	$C2/c$ (no. 15)
a / pm	663.41(4)
b / pm	873.02(5)
c / pm	905.55(8)
β / °	104.763(3)
Volume / 10^6 pm^3	507.15(6)
Z	4
ρ_{calcd} / g cm^{-3}	3.139
Absorption coefficient μ / mm^{-1}	5.10
$F(000)$ / e	468
Radiation; wavelength λ / Å	Mo$K\alpha$; 0.71073
Diffractometer	Bruker D8 Venture
θ range / °	3.942–34.978
Absorption correction	Multi-scan
Transmission (min; max)	0.6295; 0.7497
Index range $h\|k\|l$	-8;10|±14|±14
Reflections collected	7880
Independent reflections	1117
Obs. reflections ($I > 2\,\sigma(I)$)	1028
Refined parameters	48
R_{int}	0.037
R_1	0.021
wR_2	0.049
GooF	1.076
Residual electron density (max; min) / e^- Å^{-3}	0.82; -0.43

[a] The respective standard deviations are given in parentheses.

Table S11. Wyckoff symbol, atomic coordinates *x*; *y*; *z* and equivalent isotropic displacement parameters U_{eq} in Å^2 for $Cu[S_2O_7]$[a]

Atom	Wyckoff symbol	*x*	*y*	*z*	U_{eq}
Cu1	4*c*	3/4	1/4	1/2	0.0087(1)
S1	8*f*	0.67137(4)	0.10163(3)	0.18602(3)	0.0081(1)
O1	8*f*	0.8186(1)	0.1607(1)	0.3219(1)	0.0112(2)
O2	4*e*	0.5	0.0060(1)	1/4	0.0105(2)
O3	8*f*	0.5548(1)	0.2239(1)	0.0928(1)	0.0129(2)
O4	8*f*	0.7584(1)	-0.0098(1)	0.1064(1)	0.0146(2)

[a] The respective standard deviations are given in parentheses.

Table S12. Anisotropic displacement parameters U_{ij} in Å^2 for $Cu[S_2O_7]$[a]

Atom	U_{11}	U_{22}	U_{33}	U_{23}	U_{13}	U_{12}
Cu1	0.00865(9)	0.01008(9)	0.00701(10)	-0.00209(6)	0.00128(7)	-0.00113(6)
S1	0.00878(12)	0.00792(11)	0.00745(12)	-0.00126(8)	0.00154(9)	0.00023(8)
O1	0.0091(4)	0.0149(4)	0.0086(4)	-0.0033(3)	0.0008(3)	-0.0013(3)
O2	0.0107(5)	0.0076(4)	0.0140(6)	0	0.0047(4)	0
O3	0.0106(4)	0.0137(4)	0.0133(4)	0.0052(3)	0.0012(3)	0.0008(3)
O4	0.0155(4)	0.0133(4)	0.0166(5)	-0.0069(3)	0.0072(3)	0.0000(3)

[a] The respective standard deviations are given in parentheses.

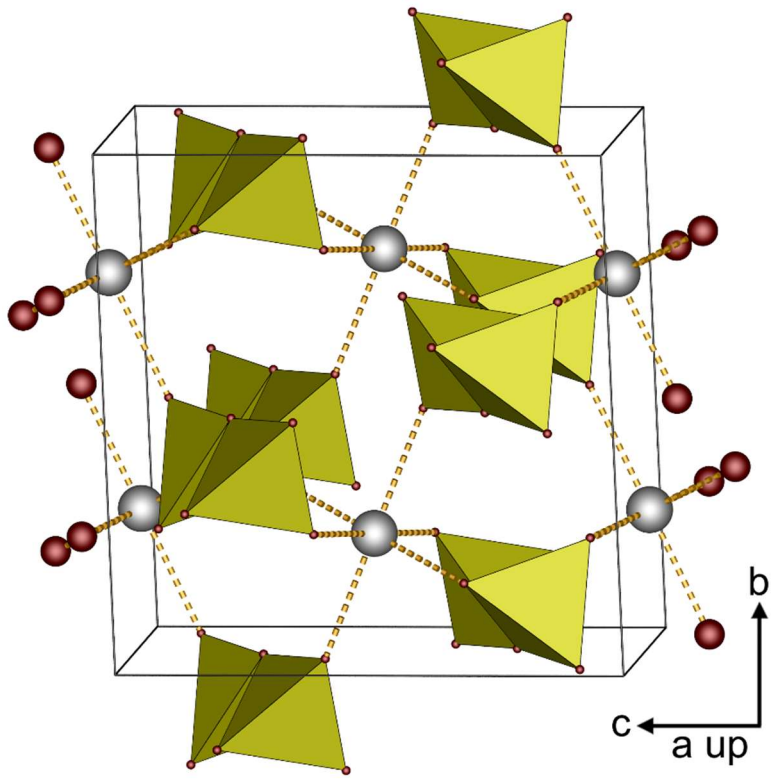

Fig. S10. Unit cell of $Cu[S_2O_7]$ viewed approximately along (100); sulfate tetrahedra yellow, copper cations grey, oxygen atoms red.

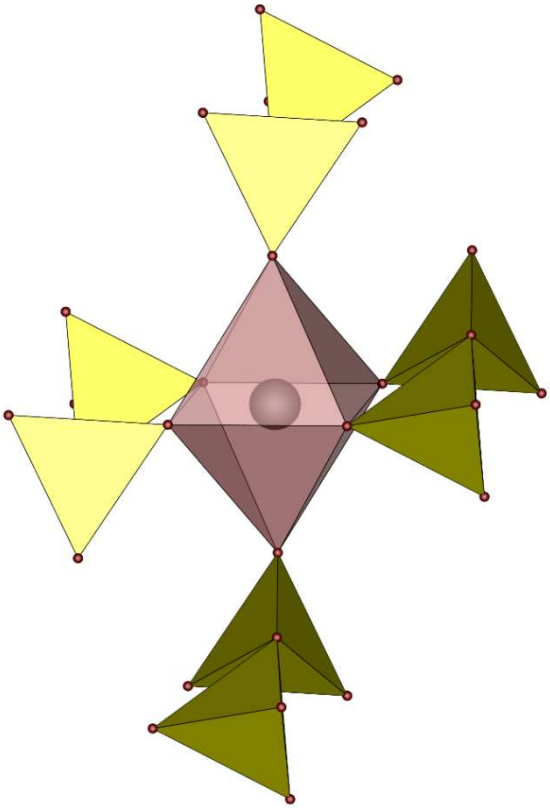

Fig. S11. Octahedral coordination environment of the Cu^{2+} cations (grey) in $Cu[S_2O_7]$; sulfate tetrahedra yellow, copper cations grey, oxygen atoms red.

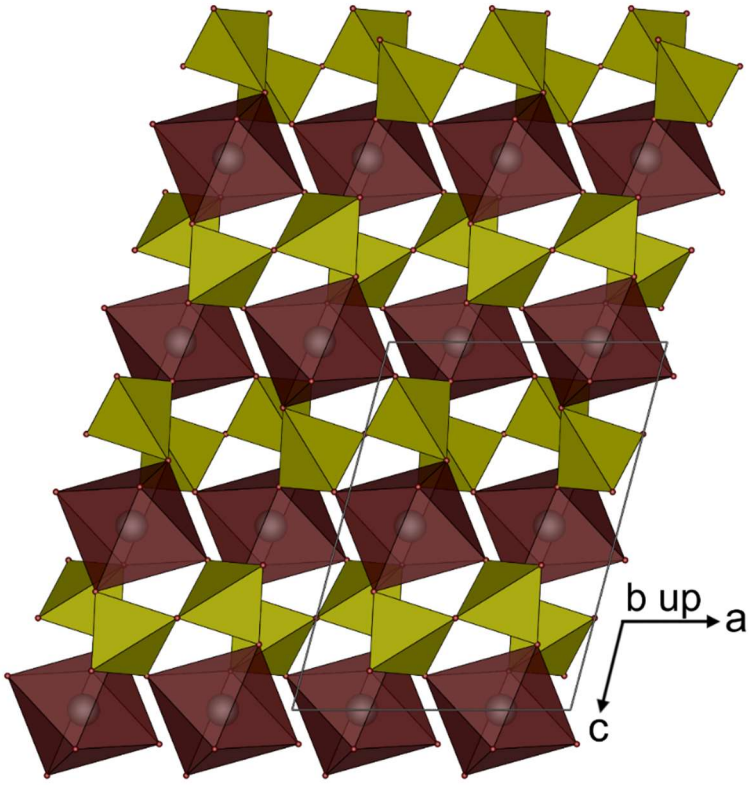

Fig. S12. Layered arrangement of Cu^{2+} cations (grey) and $[S_2O_7]^{2-}$ anions in $Cu[S_2O_7]$; sulfate tetrahedra yellow, copper cations grey, oxygen atoms red.

Table S13. Electrostatic calculations for $Cu[S_2O_7]$.

$Cu[S_2O_7]$	$CuO^4 + 2\ SO_3^2$
MAPLE = 64319 kJ mol^{-1}	MAPLE = 64486 kJ mol^{-1}
	(Δ = 0.26%)

Table S14. ECon derived by MAPLE-calculations for copper atoms in $Cu[S_2O_7]$

Atom	*x*	*y*	*z*	Distance / pm	Econ(1)	Econ(3)
Central atom						
Cu1	3/4	1/4	1/2			
Ligand						
O1	0.8186	0.1607	0.3219	194.712	1.155	1.179
O1	0.6814	0.3393	0.6782	194.712	1.155	1.179
O3	0.4452	0.2239	0.4072	199.526	1.009	1.034
O3	1.0548	0.2761	0.5928	199.526	1.009	1.034
O4	0.7584	0.0098	0.6064	230.25	0.262	0.277
O4	0.7416	0.4902	0.3936	230.25	0.262	0.277
Next Ligand						
O2	1	0.494	3/4	324.047	0	0

Table S15. Selected interatomic distances (in pm) and angles (in deg) of α-$Cu[B_2(SO_4)_4]$[a]

Cu–O11	196.3(9)
Cu–O21	188(1)
Cu–O22[b]	217.1(9)
∑ IR (Cu–O)[5]	208
S1–O	145.7(9)-160(1)
S2–O	147(1)-157(1)
∑ IR (S–O)[5]	150
B–O	143(2)-160(2)
∑ IR (B–O)[5]	149
O–S1–O	100(1)-118.7(7)
O–S2–O	102(1)-122.4(6)
O–B–O	101(1)-120(2)

[a] The respective standard deviations are given in parentheses. The data was taken from the Rietveld refinement. [b] O22 is part of the anion coordinating Cu^{2+} via one sulfate group, only.

Table S16. Electrostatic calculations α-$Cu[B_2(SO_4)_4]$ and β-$Cu[B_2(SO_4)_4]$.

α-$Cu[B_2(SO_4)_4]$ (Rietveld)		$CuSO_4$[1] + $B_2S_2O_9$[6] + SO_3[7]
MAPLE = 142636 kJ mol^{-1}		MAPLE = 142929 kJ mol^{-1}
	(Δ = 0.21%)	
β-$Cu[B_2(SO_4)_4]$ (SC-XRD)		$CuSO_4$[1] + B_2O_3[8] + 3 SO_3[2]
MAPLE = 146610 kJ mol^{-1}		MAPLE = 146832 kJ mol^{-1}
	(Δ = 0.15%)	
β-$Cu[B_2(SO_4)_4]$ (Rietveld)		$CuSO_4$[1] + B_2O_3[8] + 3 SO_3[2]
MAPLE = 146352 kJ mol^{-1}		MAPLE = 146832 kJ mol^{-1}
	(Δ = 0.33%)	

Table S17. ECon derived by MAPLE-calculations for Cu atoms in α-$Cu[B_2(SO_4)_4]$ (Rietveld)

Atom	*x*	*y*	*z*	Distance / pm	Econ(1)	Econ(3)
Central atom						
Cu1	½	½	½			
Ligand						
O21	0.5860	0.5668	0.6889	188.520	1.207	1.233
O21	0.4140	0.4332	0.3111	188.520	1.207	1.233
O11	0.4192	0.7705	0.3936	196.331	0.965	0.992
O11	0.5808	0.2295	0.6064	196.331	0.965	0.992
O22	0.0860	0.4721	0.6845	217.099	0.409	0.430
O22	0.9140	0.5279	0.3155	217.099	0.409	0.430
Next Ligand						
O111	0.7301	0.8528	0.0723	348.975	0	0

Table S18. Crystal data and structure refinements of β-Cu[$B_2(SO_4)_4$] determined from single crystal XRD[a]

CSD number	2118186
M / g mol^{-1}	469.40
Crystal size / mm^3	0.19 × 0.15 × 0.11
Temperature / K	250(2)
Space group	$P2_1/n$ (no. 14)
a / pm	771.2(3)
b / pm	814.9(3)
c / pm	909.2(3)
β / °	111.220(11)
Volume / 10^6 pm^3	532.7(4)
Z	2
ρ_{calcd} / g cm^{-3}	2.927
Absorption coefficient μ / mm^{-1}	2.94
F(000) / e	462
Radiation; wavelength λ / Å	Mo$K\alpha$; 0.71073
Diffractometer	Bruker D8 Venture
θ range / °	2.979–44.998
Absorption correction	Multi-scan
Transmission (min; max)	0.6364; 0.7503
Index range $h\|k\|l$	-14;15|±16|-18;17
Reflections collected	34144
Independent reflections	4392
Obs. reflections ($I > 2\ \sigma(I)$)	3946
Refined parameters	107
R_{int}	0.034
R_1	0.026
wR_2	0.057
GooF	1.099
Residual electron density (max; min) / e^- Å^{-3}	0.69; -0.72

[a] The respective standard deviations are given in parentheses.

Table S19. Wyckoff symbol, atomic coordinates *x*; *y*; *z* and equivalent isotropic displacement parameters U_{eq} in Å^2 for β-Cu[$B_2(SO_4)_4$][a]

Atom	Wyckoff symbol	*x*	*y*	*z*	U_{eq}
Cu1	2*a*	0	0	0	0.00930(3)
S1	4*e*	-0.70341(2)	0.07667(2)	0.35248(2)	0.00705(3)
S2	4*e*	-0.28559(2)	-0.15745(2)	0.14445(2)	0.00767(3)
O11	4*e*	-0.55572(8)	-0.00838(6)	0.30333(7)	0.00960(7)
O12	4*e*	-0.87400(8)	0.07809(8)	0.21717(6)	0.01419(9)
O13	4*e*	-0.64003(8)	0.23124(7)	0.42536(7)	0.01201(8)
O14	4*e*	-0.26681(8)	0.04578(7)	0.53145(6)	0.01036(8)
O21	4*e*	-0.25357(8)	-0.07599(8)	0.30274(7)	0.0139(1)
O22	4*e*	-0.46914(8)	-0.21492(9)	0.06907(8)	0.0169(1)
O23	4*e*	-0.35697(8)	0.20540(7)	0.29374(7)	0.01281(9)
O24	4*e*	-0.21975(9)	-0.04850(9)	0.04959(8)	0.0164(1)
B1	4*e*	-0.3588(1)	0.04135(9)	0.35691(9)	0.0083(1)

[a] The respective standard deviations are given in parentheses.

Table S20. Anisotropic displacement parameters U_{ij} in Å^2 for β-Cu[$B_2(SO_4)_4$][a]

Atom	U_{11}	U_{22}	U_{33}	U_{23}	U_{13}	U_{12}
Cu1	0.00893(5)	0.01355(5)	0.00553(4)	-0.00049(3)	0.00273(3)	-0.00231(3)
S1	0.00772(5)	0.00795(5)	0.00516(5)	-0.00063(4)	0.00193(4)	-0.00002(4)
S2	0.00727(5)	0.00943(6)	0.00715(6)	-0.00116(4)	0.00362(4)	-0.00021(4)
O11	0.00943(17)	0.00996(17)	0.01056(2)	-0.0026(1)	0.0050(1)	-0.0006(1)
O12	0.01087(19)	0.0216(3)	0.0071(2)	-0.0026(2)	-0.0003(2)	0.0031(23)
O13	0.0147(2)	0.0082(2)	0.0134(2)	-0.0027(2)	0.0054(2)	-0.0011(2)
O14	0.01372(19)	0.0113(2)	0.0067(2)	-0.0005(1)	0.0044(1)	-0.0035(2)
O21	0.0136(2)	0.0183(2)	0.0096(2)	-0.0048(2)	0.0038(2)	0.0053(2)
O22	0.00930(19)	0.0213(3)	0.0185(2)	-0.0042(2)	0.0032(2)	-0.0041(2)
O23	0.0137(2)	0.0102(2)	0.0128(2)	0.0033(1)	0.0027(2)	-0.0034(2)
O24	0.0137(2)	0.0219(3)	0.0162(2)	0.0082(2)	0.0085(2)	0.0009(2)
B1	0.0101(2)	0.0083(2)	0.0077(2)	-0.0002(2)	0.0047(2)	-0.00002(19)

[a] The respective standard deviations are given in parentheses.

Table S21. Selected interatomic distances (in pm) and angles (in deg) of β-$Cu[B_2(SO_4)_4]$[a]

	SC-XRD	Rietveld
Cu–O12	196.48(8)	203.6(7)
Cu–O13	242.8(1)	239.4(8)
Cu–O24	195.54(9)	189.5(8)
∑ IR (Cu–O)[5]	208	208
S1–O[b]	142.51(7)-153.14(7)	140.0(8)-154.9(9)
S2–O	141.06(8)-152.56(7)	135.7(8)-155.5(8)
∑ IR (S–O)[5]	150	150
B–O	145.1(1)-148.5(1)	139(2)-157(2)
∑ IR (B–O)[5]	149	149
O–S1–O	102.67(4)-116.35(4)	101.1(5)-117.9(4)
O–S2–O	97.04(4)-114.82(5)	92.6(4)-118.5(5)
O–B–O	105.59(6)-113.36(6)	101(1)-118(1)

[a] The respective standard deviations are given in parentheses. [b] $S1O_4$ tetrahedra are forming the *vierer* Rings.

Table S22. Deviation from the ideal symmetry Δ_{octa} or Δ_{tetr} (in %) for α-$Cu[B_2(SO_4)_4]$ and β-$Cu[B_2(SO_4)_4]$ and distance of the Cu^{2+} cation from the centroid of the octahedron calculated by the method of Balic-Zunic and Makovicky on experimental data.[9]

	α-$Cu[B_2(SO_4)_4]$ (Rietveld)	β-$Cu[B_2(SO_4)_4]$ (SC-XRD)	β-$Cu[B_2(SO_4)_4]$ (Rietveld)
Δ_{octa} ($Cu1O_6$)	21.96	35.41	33.1
Δ_{tetr} ($B1O_4$)	0.72	0.44	0.66
Δ_{tetr} ($S1O_4$)[a]	1.17	0.17	1.04
Δ_{tetr} ($S2O_4$)	1.81	0.65	1.31
Distance from centroid ($Cu1O_6$)	0.017 pm	0.018 pm	0.0089 pm

[a] $S1O_4$ tetrahedra are forming the *Vierer* Rings in α-$Cu[B_2(SO_4)_4]$.

Table S23. ECon derived by MAPLE-calculations for Cu atoms in β-$Cu[B_2(SO_4)_4]$ (SC-XRD)

Atom	*x*	*y*	*z*	Distance / pm	Econ(1)	Econ(2)
Central atom						
Cu1	0	½	0			
Ligand						
O24	0.2197	0.5485	-0.0496	194.543	1.073	1.082
O24	-0.2197	0.4515	0.0496	194.543	1.073	1.082
O12	-0.1260	0.4219	-0.2172	196.437	1.015	1.024
O12	0.1260	0.5781	0.2172	196.437	1.015	1.024
O13	-0.1400	0.7688	-0.0746	242.760	0.081	0.084
O13	0.1400	0.2312	0.0746	242.760	0.081	0.084
Next Ligand						
O23	0.1430	0.7946	-0.2063	346.336	0	0

Table S24. ECon derived by MAPLE-calculations for Cu atoms in β-$Cu[B_2(SO_4)_4]$ (Rietveld)

Atom	*x*	*y*	*z*	Distance / pm	Econ(1)	Econ(2)
Central atom						
Cu1	0	0	0			
Ligand						
O24	0.2120	0.0434	-0.0522	189.484	1.200	1.241
O24	-0.2120	-0.0434	0.0522	189.484	1.200	1.241
O12	-0.1273	-0.0779	-0.2270	203.586	0.773	0.814
O12	0.1273	0.0779	0.2270	203.586	0.773	0.814
O13	-0.1363	0.2664	-0.0714	239.352	0.098	0.112
O13	0.1363	-0.2664	0.0714	239.352	0.098	0.112
Next Ligand						
O23	0.1426	0.2968	-0.2161	352.611	0	0

Table S25. Optimized lattice parameters and cell volumes per formula unit for α-$Cu[B_2(SO_4)_4]$ (*P*-1), β-$Cu[B_2(SO_4)_4]$ (*P*2_1/*n*) and a hypothetical γ-$Cu[B_2(SO_4)_4]$ (*C*2/*c*, "cation between layer"); note that space group setting here is *P*2_1/*c* for β-$Cu[B_2(SO_4)_4]$

	a / Å	*b* / Å	*c* / Å	α / °	β / °	γ / °	$V\ Z^{-1}$ / Å^3
α-$Cu[B_2(SO_4)_4]$	5.292	7.359	8.035	73.48	71.05	86.13	283.63
β-$Cu[B_2(SO_4)_4]$	7.673	8.449	9.647		116.29		280.36
"γ-$Cu[B_2(SO_4)_4]$"	17.662	5.336	14.541		125.06		280.46

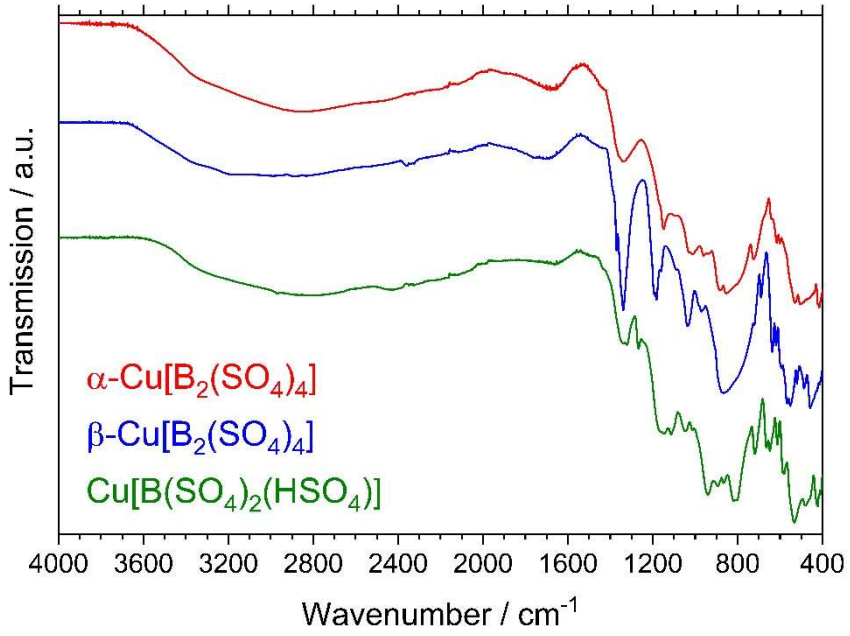

Fig. S13. Full infrared spectra of α-$Cu[B_2(SO_4)_4]$, β-$Cu[B_2(SO_4)_4]$ and $Cu[B(SO_4)_2(HSO_4)]$ including broad bands at high wavelengths that can be assigned to O-H vibrations (centred at 2800cm^{-1} and 1700cm^{-1}) presumably related to the formation of sulfuric acid on the surface of the samples reacting with ambient moisture.[10]

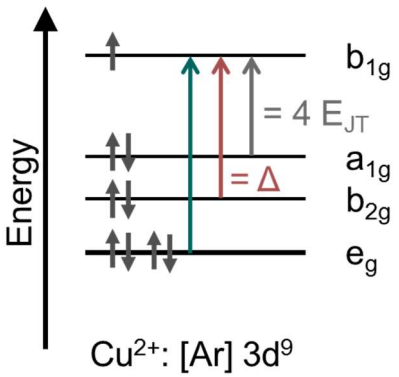

Fig. S14. Cu^{2+} energy scheme in D_{4h} symmetry showing the three possible d-d transitions of Cu^{2+} and the related parameters according to classical ligand field theory (Δ: ligand field splitting energy, E_{JT}: Jahn-Teller energy)

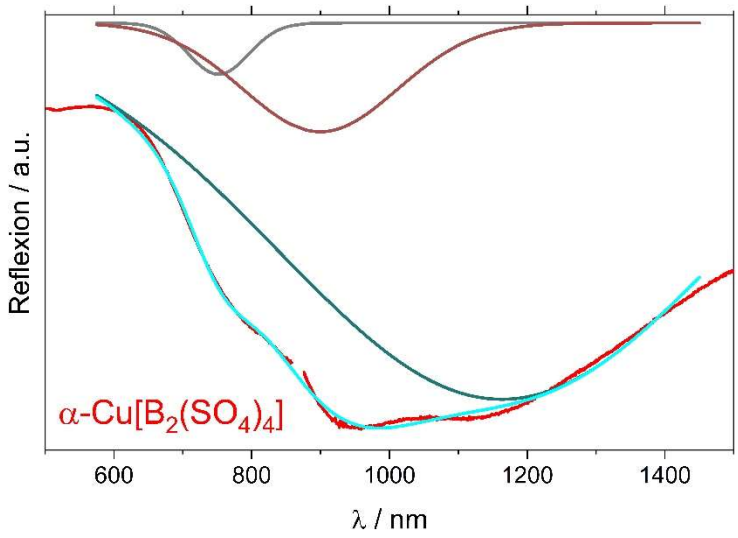

Fig. S15. Gaussian fit of the UV-Vis-NIR spectrum of α-$Cu[B_2(SO_4)_4]$

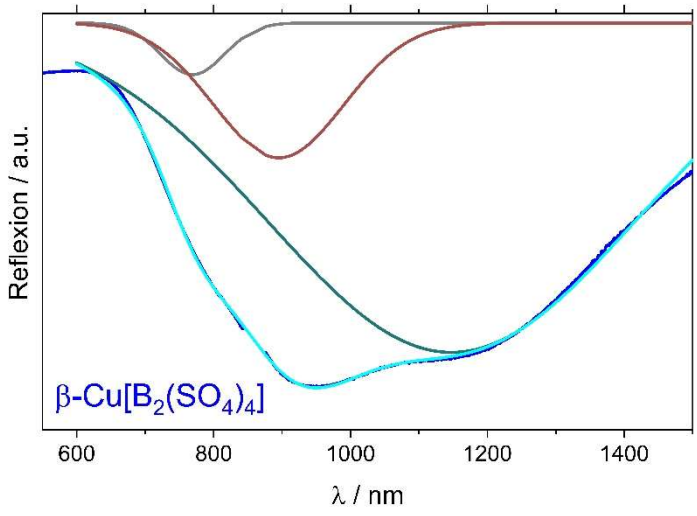

Fig. S16. Gaussian fit of the UV-Vis-NIR spectrum of β-$Cu[B_2(SO_4)_4]$

Table S26. Comparison of relevant parameters derived from the UV-Vis-NIR spectra of $Cu[B_2(SO_4)_4]$ and $Cu[B(SO_4)_2(HSO_4)]$ with other Cu^{2+} compounds from literature

Compound	E_{JT} / cm^{-1}	Δ / cm^{-1}	Δ_{oct} / %	$T = R_{eq}/R_{aq}$	Reference
α-$Cu[B_2(SO_4)_4]$	2149	11116	22 / 28[a]	0.89 / 0.85[a]	this work / 11
β-$Cu[B_2(SO_4)_4]$	2179	11171	33 / 35[a]	0.82 / 0.81[a]	this work
$Cu[B(SO_4)_2(HSO_4)]$	2447	12355	44 / 34[b]	0.79	this work[c]
$CuSO_4$	1830	9100	26	0.84	1,12
$CuWO_4$	2319	11136	32	0.82	13
$CsCuCl_3$	2076	10000	26	0.83	14
K_2CuF_4	1950	9200	25	0.87	15
$[Cu^{II}[OH_2)_6]^{2+}$	~2000	~13000	-		16

[a] Results using Rietveld on the left and single-crystal data on the right. [b] There are two crystallographically distinct CuO_6 polyhedra in $Cu[B(SO_4)_2(HSO_4)]$. [c] Δ_{oct} and T were calculated using the single-crystal data reported by Bruns et. al.[11]

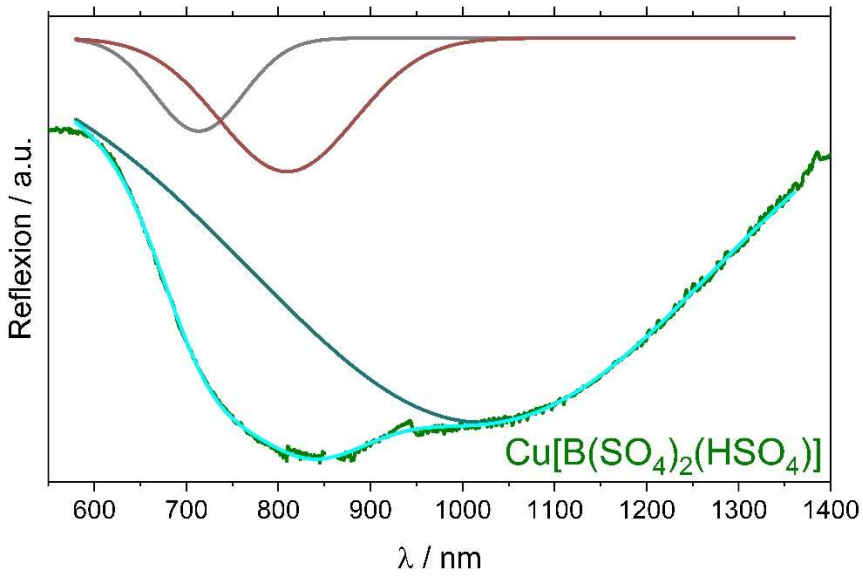

Fig. S17. Gaussian fit of the UV-Vis-NIR spectrum of $Cu[B(SO_4)_2(HSO_4)]$

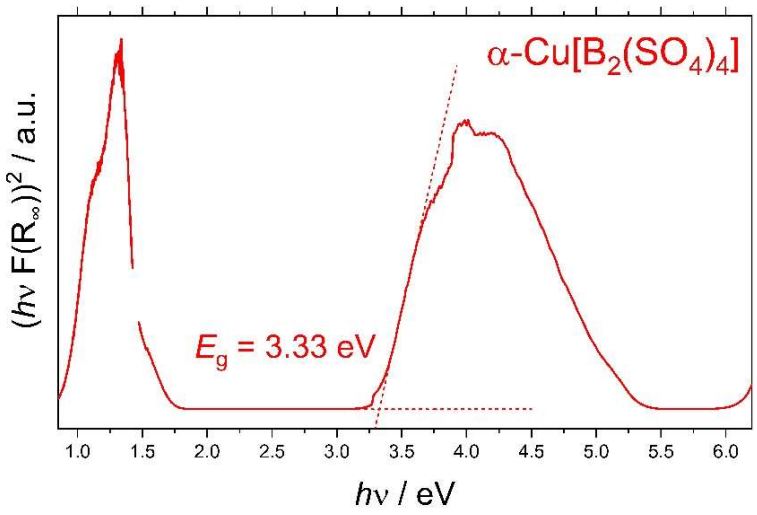

Fig. S18. Tauc plot calculated from the UV-Vis-NIR spectrum of α-Cu[$B_2(SO_4)_4$] assuming a direct band gap

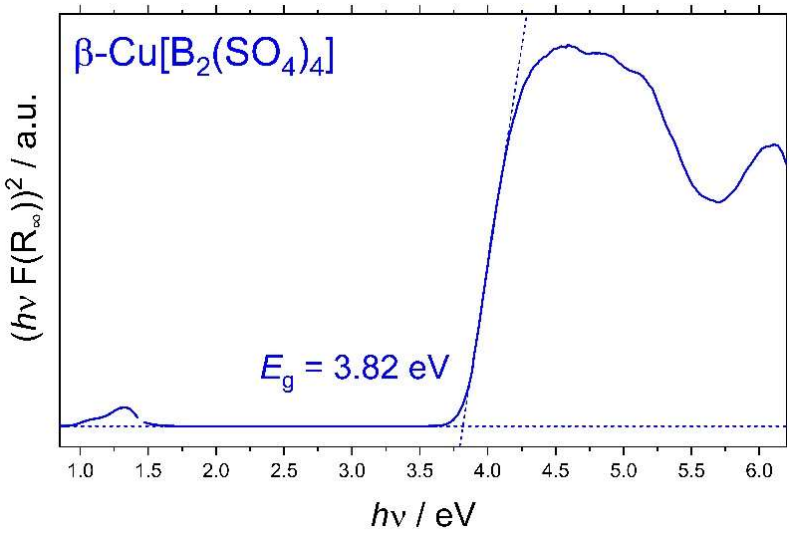

Fig. S19. Tauc plot calculated from the UV-Vis-NIR spectrum of β-Cu[$B_2(SO_4)_4$] assuming a direct band gap

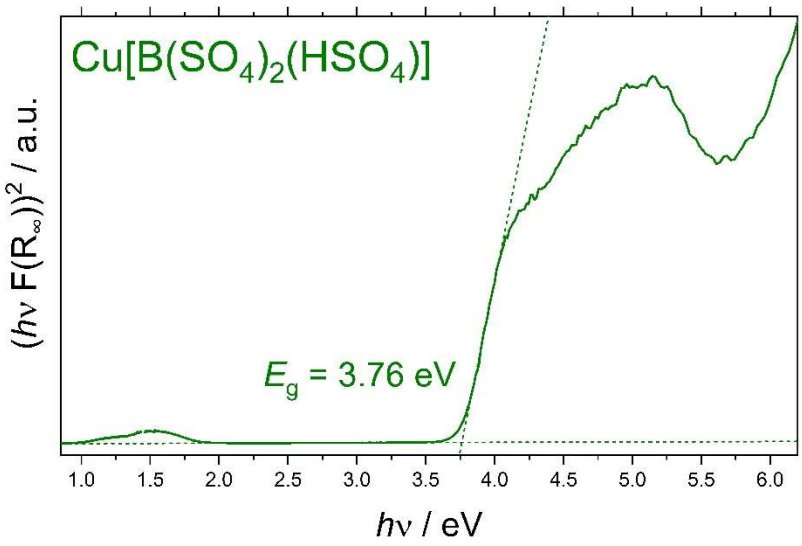

Fig. S20. Tauc plot calculated from the UV-Vis-NIR spectrum of $Cu[B(SO_4)_2(HSO_4)]$ assuming a direct band gap

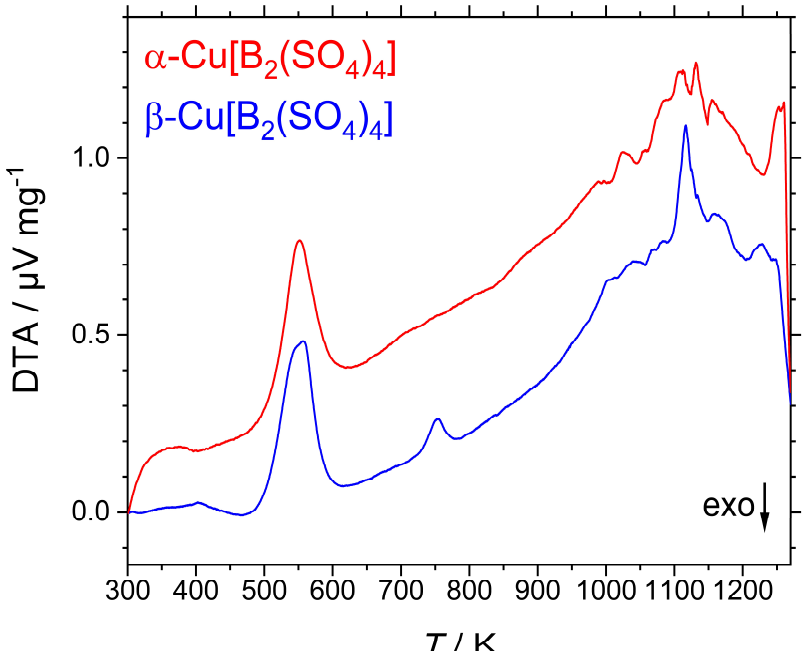

Fig. S21. Differential thermal analyses of α-$Cu[B_2(SO_4)_4]$ and β-$Cu[B_2(SO_4)_4]$ measured simultaneously with the thermogravimetric data displayed in Fig. 6.

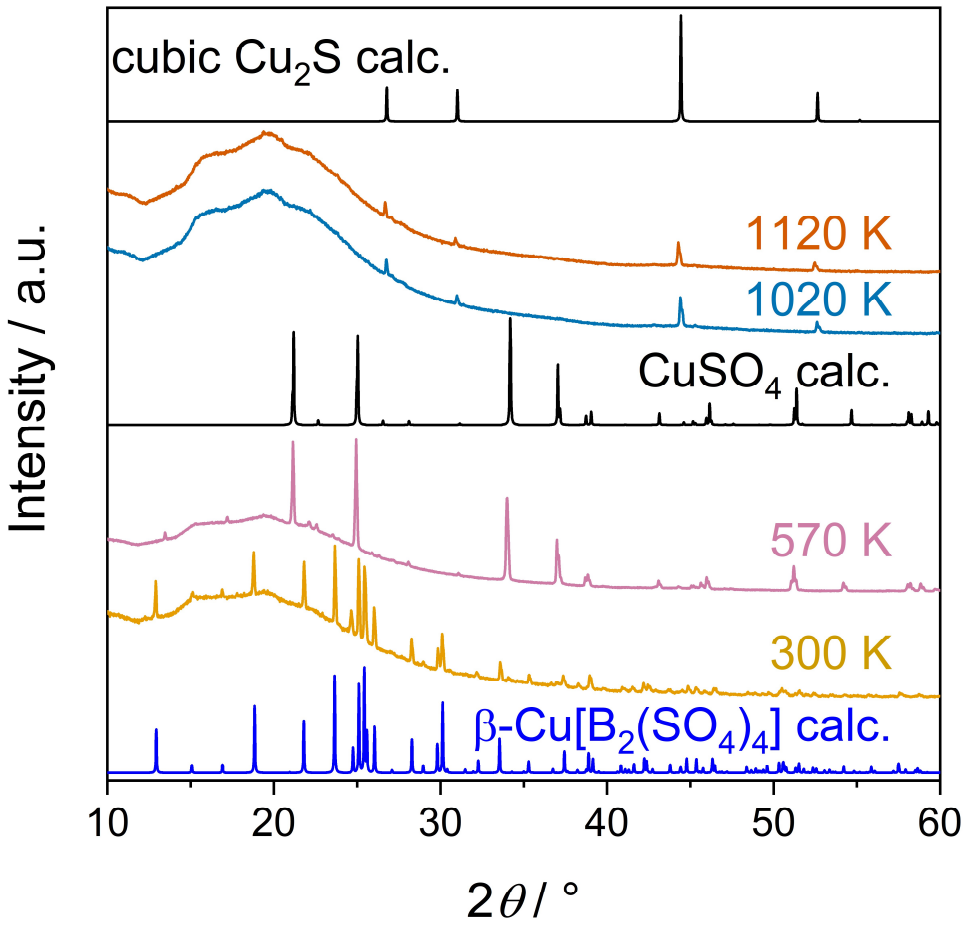

Fig. S22. TPXRD powder pattern of β-$Cu[B_2(SO_4)_4]$ compared to calculated patterns for β-$Cu[B_2(SO_4)_4]$ from our single-crystal XRD, $CuSO_4$[1] and cubic Cu_2S[17] confirming the latter two as decomposition products of the former.

Table S27. Experimental and theoretically predicted mass losses in wt.-% for the thermogravimetric analysis of $Cu[B_2(SO_4)_4]$ depicted in Fig. 6

Decomposition Step	TGA α	TGA β	avg.*	Theory
$Cu[B_2(SO_4)_4] \rightarrow CuSO_4 + B_2O_3 + 3SO_3(g)$ + adhesive* (g)	53.3	52.2	51.3	51.2
$CuSO_4 + B_2O_3 \rightarrow \frac{1}{3}\ CuO + \frac{2}{3}\ Cu(SO_4) + B_2O_3 + \frac{1}{3}\ SO_3(g)$	58.8	58.1	57.0	57.0
$\frac{1}{3}\ CuO + \frac{2}{3}\ Cu(SO_4) + B_2O_3 \rightarrow CuO + B_2O_3 + \frac{2}{3}\ SO_3(g)$	70.1	69.3	68.2	68.2

*average values corrected for an inital loss of approx. 1.5% of adhesive liquid (H_2SO_4, b.p. 553 K)

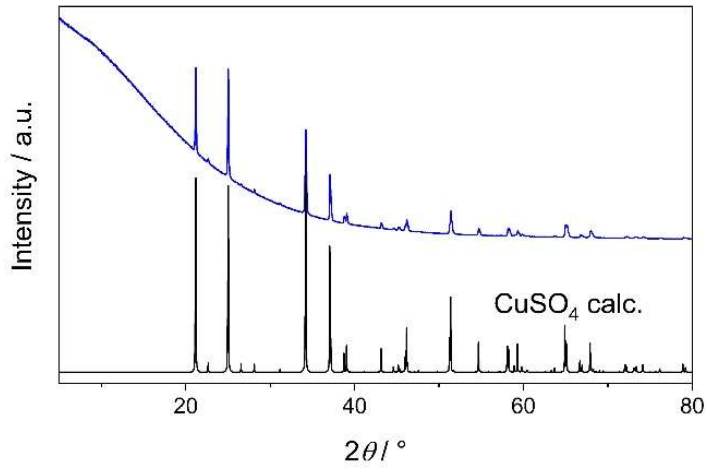

Fig. S23. Powder XRD pattern of β-Cu[$B_2(SO_4)_4$] heated at 573 K for 10 h in nitrogen atmosphere compared to a calculated pattern for $CuSO_4$.[1]

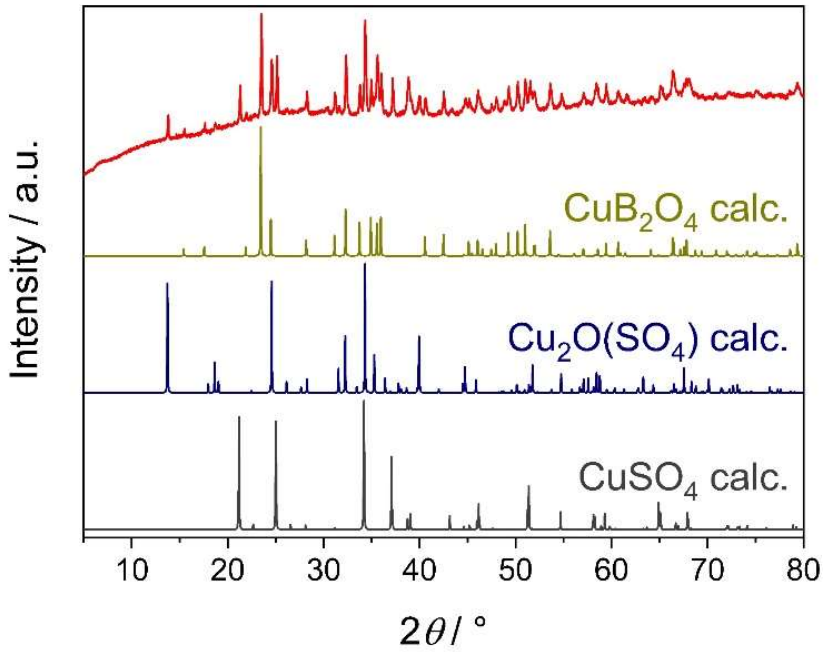

Fig. S24. Powder XRD pattern of α-Cu[$B_2(SO_4)_4$] heated for 10 h at 973 K in ambient air compared to calculated pattern for $CuSO_4$,[1] $Cu_2O(SO_4)$[18] and CuB_2O_4.[19]

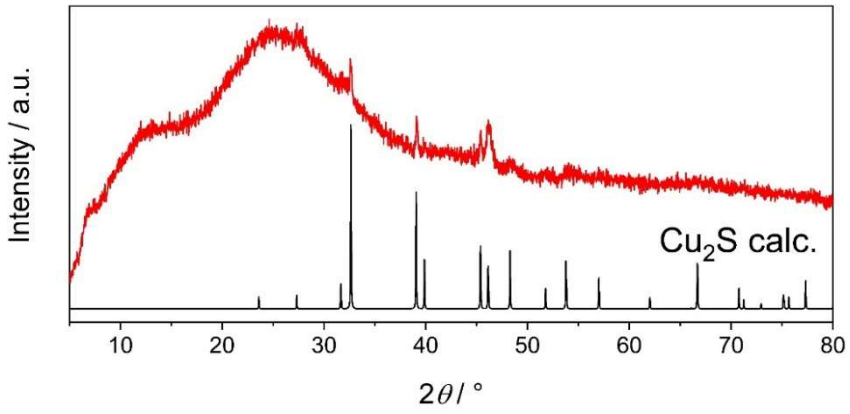

Fig. S25. Powder XRD pattern of decomposed α-Cu[$B_2(SO_4)_4$] after the TG/DTA measurement compared to a calculated pattern for tetragonal Cu_2S.[20]

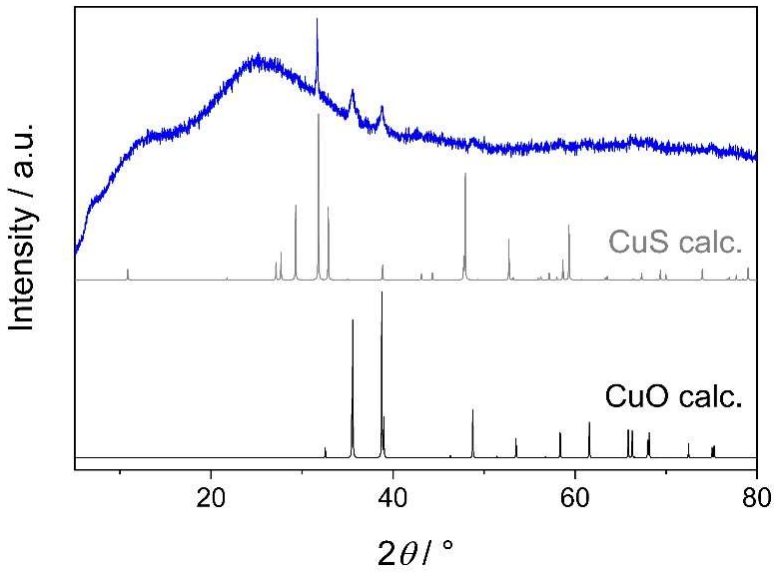

Fig. S26. Powder XRD pattern of β-Cu[$B_2(SO_4)_4$] heated at 1273 K for 10 h in ambient air compared to calculated pattern for CuS[21] and CuO.[22]

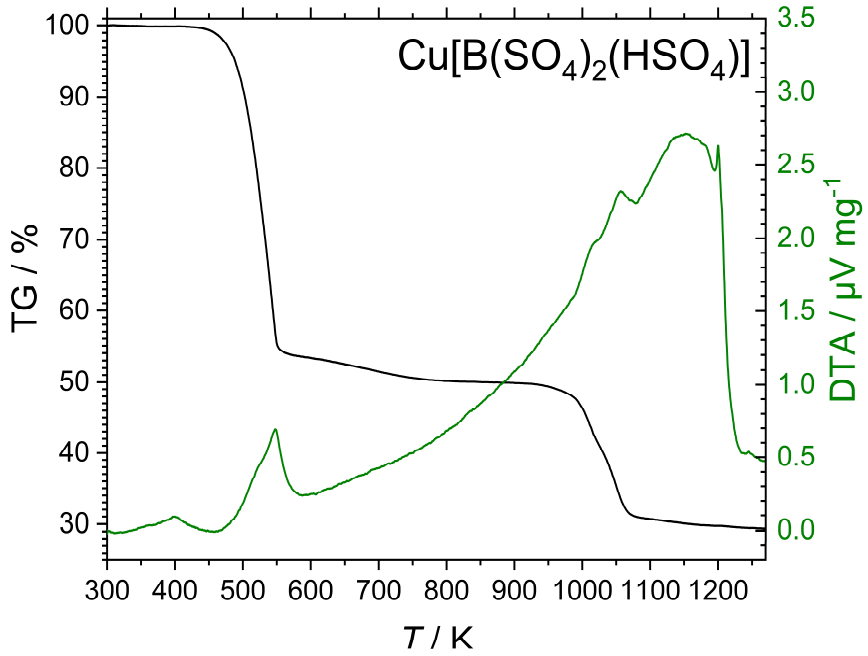

Fig. S27. Thermogravimetric and differential thermal analysis of Cu[$B(SO_4)_2(HSO_4)$].

Table S28. Experimental and theoretically predicted mass losses in wt.-% for the thermogravimetric analysis of Cu[$B(SO_4)_2(HSO_4)$] depicted in Fig. S27

Decomposition Step	TGA	Theory
Cu[$B(SO_4)_2(HSO_4)$]→ $CuSO_4$ + ½ B_2O_3 + 2SO_3(g) + ½ H_2O(g)	46.5	46.5
$CuSO_4$ + B_2O_3 → ½ $Cu_2O(SO_4)$ + ½ B_2O_3 + ½ SO_3(g)	58.7	57.5
½ $Cu_2O(SO_4)$ + B_2O_3 → ½ Cu_2S + ½ B_2O_3 + ½ SO_3(g) + ½ O_2(g)	69.0	68.5

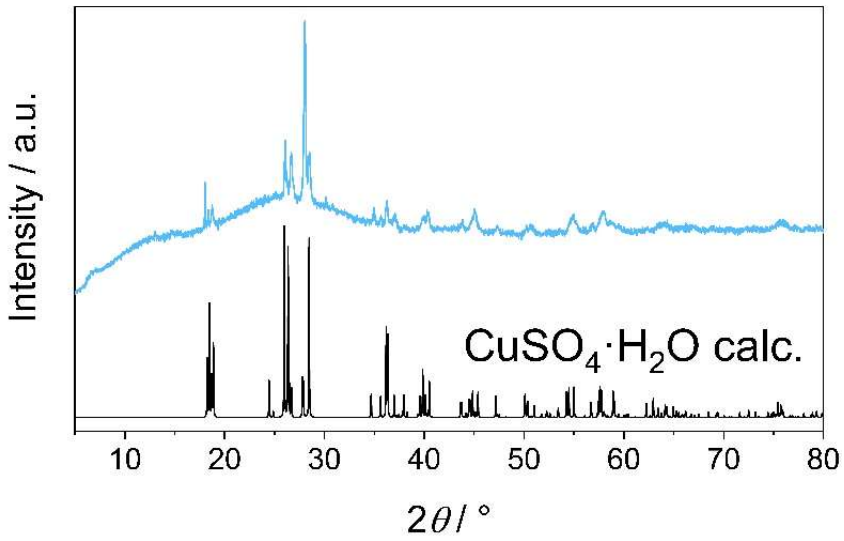

Fig. S28. Powder XRD pattern of β-$Cu[B_2(SO_4)_4]$ stored at ambient conditions for 30 min compared to a calculated pattern for $CuSO_4 \cdot H_2O$.[23]

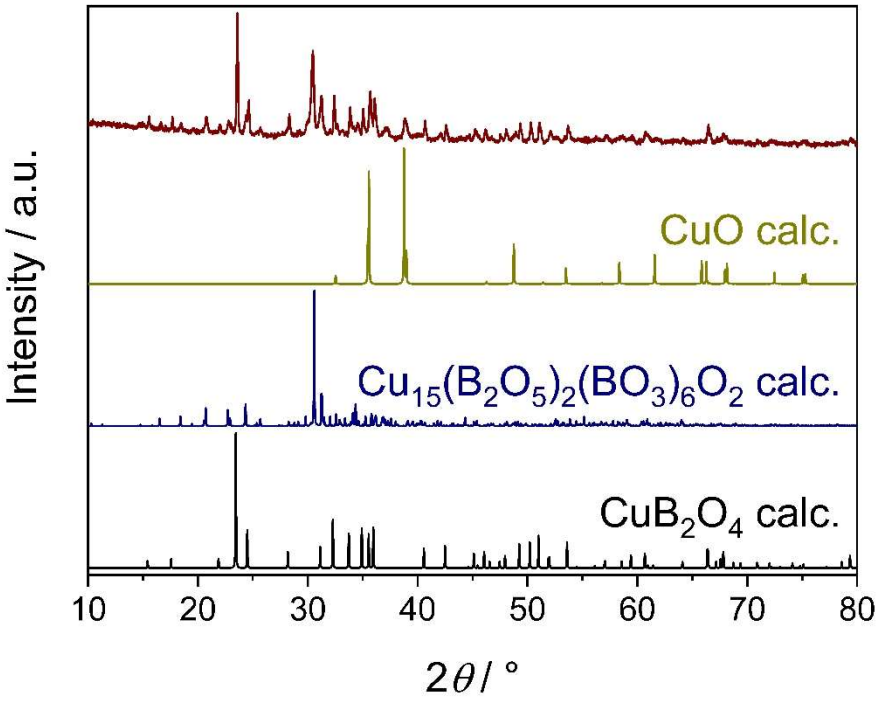

Fig. S29. Powder XRD pattern of the educt used for the synthesis of $Cu[S_2O_7]$ compared to calculated patterns for CuB_2O_4,[24] $Cu_3B_2O_6$ or $Cu_{15}(B_2O_5)_2(BO_3)_6O_2$[25] and CuO.[22]

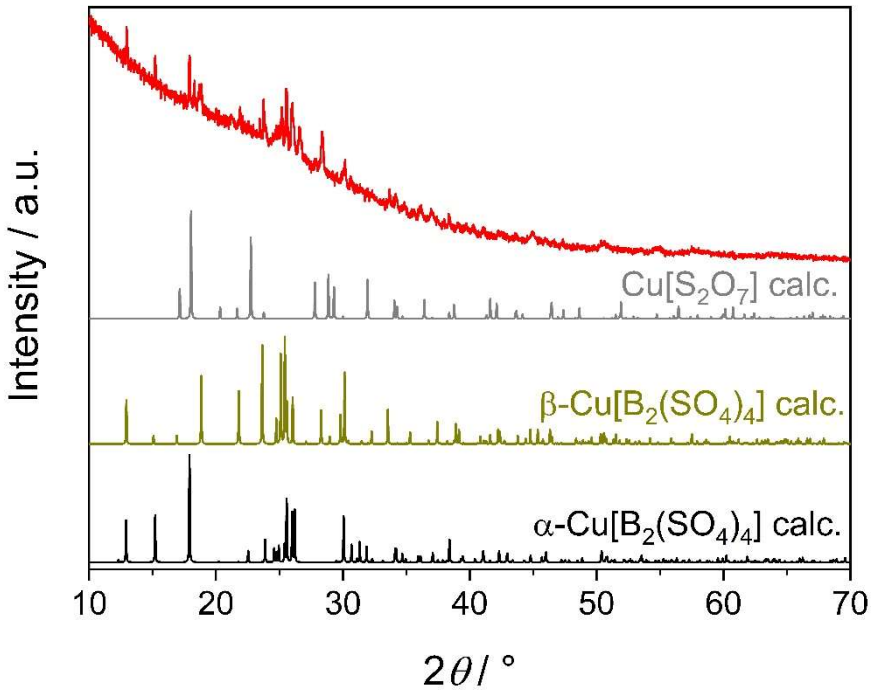

Fig. S30. Powder XRD pattern of the sample containing the $Cu[S_2O_7]$ single crystals after the washing step compared to calculated patterns for $Cu[S_2O_7]$ and β-$Cu[B_2(SO_4)_4]$ from our single-crystal data and for α-$Cu[B_2(SO_4)_4]$.[11]

References

1 M. Wildner and G. Giester, *Miner. Petrol.*, 1988, **39**, 201–209.
2 R. Pascard and C. Pascard-Billy, *Acta Crystallogr.*, 1965, **18**, 830–834.
3 A. Goto, T. Hondoh and S. Mae, *J. Chem. Phys.*, 1990, **93**, 1412–1417.
4 S. Åsbrink and A. Waskowska, *J. Phys.: Condens. Matter*, 1991, **3**, 8173–8180.
5 R. D. Shannon, *Acta Crystallogr. A*, 1976, **32**, 751–767.
6 C. Logemann and M. S. Wickleder, *Angew. Chem. Int. Ed.*, 2013, **52**, 14229–14232.
7 R. Westrik and C. H. Mac Gillavry, *Recl. Trav. Chim. Pays-Bas*, 1941, **60**, 794–810.
8 G. E. Gurr, P. W. Montgomery, C. D. Knutson and B. T. Gorres, *Acta Crystallogr. B*, 1970, **26**, 906–915.
9 a) E. Makovicky and T. Balić-Žunić, *Acta Crystallogr.*, 1998, **B54**, 766–773; b) T. Balić Žunić and E. Makovicky, *Acta Crystallogr.*, 1996, **B52**, 78–81.
10 a) K. L. Nash, K. J. Sully and A. B. Horn, *J. Phys. Chem. A*, 2001, **105**, 9422–9426; b) A. B. Horn and K. Jessica Sully, *Phys. Chem. Chem. Phys.*, 1999, **1**, 3801–3806.
11 J. Bruns, M. Podewitz, K. R. Liedl, O. Janka, R. Pöttgen and H. Huppertz, *Angew. Chem. Int. Ed.*, 2018, **57**, 9548–9552.
12 M. Wildner, G. Giester, M. Kersten and K. Langer, *Phys Chem Minerals*, 2014, **41**, 669–680.
13 J. Ruiz-Fuertes, M. N. Sanz-Ortiz, J. González, F. Rodríguez, A. Segura and D. Errandonea, *J. Phys.: Conf. Ser.*, 2010, **215**, 12048.
14 R. Laiho, M. Natarajan and M. Kaira, *Phys. Stat. Sol. (a)*, 1973, **15**, 311–317.
15 a) M. Hidaka, K. Inoue, I. Yamada and P. J. Walker, *Physica B+C*, 1983, **121**, 343–350; b) D. Oelkrug, *Structutal and Bonding*, 1971, **9**, 1.
16 a) M. A. Hitchman and T. D. Waite, *Inorg. Chem.*, 1976, **15**, 2150–2154; b) B. N. Figgis and M. A. Hitchman, *Ligand field theory and its applications*, Wiley-VCH, New York, NY, 2000.
17 G. Will, E. Hinze and A. R. M. Abdelrahman, *Eur. J. Mineral.*, 2002, **14**, 591–598.
18 E. Flügel-Kahler, *Acta Crystallogr.*, 1963, **16**, 1009–1014.
19 M. Martinez-Ripoll, S. Martínez-Carrera and S. García-Blanco, *Acta Crystallogr. B*, 1971, **27**, 677–681.
20 A. Janosi, *Acta Crystallogr.*, 1964, **17**, 311–312.
21 H. T. Evans and J. A. Konnert, *Amer. Min.*, 1976, **61**, 996–1000.
22 S. Åsbrink and L. J. Norrby, *Acta Crystallogr. B*, 1970, **26**, 8–15.
23 G. Giester, *Miner. Petrol.*, 1988, **38**, 277–284.
24 M. Martinez-Ripoll, S. Martínez-Carrera and S. García-Blanco, *Acta Crystallogr. B*, 1971, **27**, 677–681.
25 H. Behm, *Acta Crystallogr. B*, 1982, **38**, 2781–2784.